JOURNAL OF GEOSPACE SCIENCE

Vol. 4 No. 1 (2024)

E-ISSN : 2413-6093
https://jogss.org

ROLE OF CHORUS WAVES IN ENERGETIC ELECTRON ACCELERATION IN THE OUTER RADIATION BELT

Dr. Saira Najeeb

Institute of Space Science and Technology, University of Karachi, Pakistan.

Abstract

Chorus waves, a type of whistler-mode plasma wave, play a pivotal role in the dynamics of the outer radiation belt by accelerating seed electrons to relativistic energies. This article presents a comprehensive investigation of the generation, propagation, and interaction of chorus waves with energetic electrons during geomagnetic storm events. Using data from the Van Allen Probes and THEMIS missions, combined with statistical modeling and wave-particle interaction theory, we show that chorus wave amplification in the post-midnight sector is responsible for significant electron flux enhancements. The findings are supported by observational correlations, phase space density reconstruction, and local pitch-angle diffusion coefficient analysis. These results underscore the importance of chorus waves in radiation belt dynamics and contribute to improved space weather forecasting models.

OPEN ACCESS

Keywords: Chorus Waves., Radiation Belt Electrons, Wave-Particle Interactions, Magnetospheric Storms.

INTRODUCTION

The outer Van Allen radiation belt, located between 3–7 Earth radii (Re), is highly dynamic and subject to dramatic changes in response to geomagnetic activity. One of the central mechanisms governing electron flux variations in this region is the interaction with whistler-mode chorus waves. These waves, typically generated near the magnetic equator in the dawn sector, can accelerate electrons from keV to MeV energies through gyroresonant interactions [1][2].

Previous studies have shown strong spatial-temporal correlations between enhanced chorus wave activity and outer belt electron flux intensification during storms [3][4]. This study aims to extend these findings with focused analysis on Pakistani ground stations and global satellite missions, offering region-specific insights and modeling contributions.

2. Data and Methodology

To investigate the relationship between chorus waves and energetic electron acceleration in the outer radiation belt, a combination of satellite-based, ground-based, and model-driven data analysis techniques was employed.

Satellite Sources: Data were sourced from multiple spaceborne missions. The Van Allen Probes (EMFISIS instrument) provided high-resolution magnetic field wave spectra critical for identifying chorus wave activity [5]. Complementary electron flux measurements were obtained from THEMIS and GOES satellite constellations, which offered multisatellite coverage across various L-shells and magnetic local times (MLTs) [6].

Ground-Based Observations: Magnetometer data from SUPARCO-operated stations in Karachi and Islamabad were analyzed to identify Ultra-Low Frequency (ULF) wave signatures potentially modulating or coexisting with chorus wave activity [7]. This provided context for distinguishing between various wave-particle interaction regimes.

Wave and Particle Data: Chorus wave amplitudes were extracted from RBSP datasets, while electron phase space density (PSD) and pitch-angle distributions were computed from particle spectrometer readings. These were crucial for identifying regions and times of significant wave-particle resonance [8].

Modeling and Analytical Framework: A quasi-linear diffusion theory approach was applied to quantify local acceleration effects. Diffusion coefficients were derived as a function of wave power, energy, and pitch angle, incorporating L-shell resolved statistical models [9]. The analysis further included correlation matrices between chorus wave power and changes in PSD, enabling a robust evaluation of acceleration mechanisms [10].

3. Chorus Wave Generation and Propagation

Chorus waves are predominantly whistler-mode electromagnetic emissions that play a pivotal role in the local acceleration of electrons in the outer radiation belt. Their generation is closely tied to substorm-driven injections of anisotropic electron populations into the inner magnetosphere.
Excitation Mechanism: Chorus waves are generated through cyclotron resonance with anisotropic electron distributions (i.e., T⊥>T∥T_{\perp} > T_{\parallel}T⊥>T∥) injected during substorm activity. These freshly injected electrons exhibit temperature anisotropy, which leads to wave amplification under specific conditions [11].

Resonance Condition: The excitation satisfies the cyclotron resonance condition:

ω−k∥v∥=nΩe\omega - k_{\parallel}v_{\parallel} = n\Omega_eω−k∥v∥=nΩe

where ω\omegaω is the wave frequency, k∥k_{\parallel}k∥ is the parallel wave vector, v∥v_{\parallel}v∥ is the parallel electron velocity, nnn is the harmonic number (typically n=1n = 1n=1), and Ωe\Omega_eΩe is the electron gyrofrequency. This condition governs the energy and pitch-angle range of electrons that can interact with the waves [12].

Propagation Characteristics: Chorus waves predominantly propagate along geomagnetic field lines in the post-midnight to dawn magnetic local time (MLT) sector, often at L-shells between 4 and 7. The propagation characteristics are illustrated in Figure 1, which depicts their spatial localization relative to Earth's magnetic field geometry.

Controlling Factors: The ambient plasma density, magnetic field intensity, and geomagnetic activity levels influence both the growth rate and spatial extent of chorus waves. Higher plasma densities tend to suppress wave growth, while enhanced magnetic gradients can guide wave trajectories along field-aligned directions [13].

4. Wave–Particle Interaction Mechanisms

Chorus waves play a central role in the local acceleration and transport of energetic electrons in the outer radiation belt through various resonant interactions. These mechanisms enable both energy gain and spatial redistribution of particles, profoundly influencing radiation belt dynamics.

Gyroresonant Acceleration: Energetic electrons gain energy via gyroresonance, wherein they interact with the wave electric field in phase over successive gyro orbits. This cumulative process allows efficient acceleration of electrons from tens to hundreds of keV up to MeV energies, especially under sustained substorm conditions [14].

Pitch-Angle Scattering: Chorus waves also induce pitch-angle diffusion, redistributing electrons between equatorial and loss-cone pitch angles. This can lead either to trapping or precipitation into the atmosphere, depending on the resonance geometry and wave intensity. Such scattering processes help regulate the population of trapped electrons [15].

Efficiency Range and Spatial Domain: The effectiveness of chorus-induced interactions is maximized in the L = 4–6 region, corresponding to the outer radiation belt's core. Energetic electrons in the 100 keV to 1 MeV range show the strongest interaction rates, particularly during geomagnetically active periods, as shown in Figure 2 [16].

5. Case Study: April 2017 Geomagnetic Storm

The geomagnetic storm of April 21–23, 2017 offers a well-documented instance of chorus wave–driven energetic electron acceleration. It provides clear observational evidence of wave–particle interactions leading to rapid enhancements in outer belt electron flux.

Storm Intensity and Substorm Activity: The storm, characterized by a Dst index minimum of approximately –140 nT, was accompanied by intense and sustained substorm activity. These substorms injected energetic electrons with temperature anisotropies favorable for chorus wave growth [17].

Chorus Wave Power and Spatial Distribution: During the storm's main and early recovery phases, chorus wave amplitudes peaked in the dawnside magnetosphere (magnetic local time ~04–07 MLT). As shown in Figure 2, this increase coincided with a strong enhancement in phase space density (PSD) at L = 5.5, indicative of efficient in situ acceleration.

Electron Flux Enhancement: Measurements from Van Allen Probe B revealed a threefold increase in >1 MeV electron flux within 24 hours following the peak of chorus wave activity. This rapid energization aligns with model predictions of local acceleration due to wave–particle resonance [17].

6. Statistical Modeling and Diffusion Coefficients

To quantify the impact of chorus waves on electron acceleration, we applied statistical modeling techniques and diffusion theory to observational datasets. These analyses helped estimate resonance-driven transport rates and validate empirical relationships between wave power and energetic electron enhancements.

Pitch-Angle Diffusion Coefficients: Using wave amplitude measurements from RBSP (Radiation Belt Storm Probes), we derived local pitch-angle diffusion coefficients DααD_{\alpha\alpha}Dαα under the quasi-linear approximation. These coefficients characterize the rate at which electrons are scattered in pitch angle, a key parameter governing both acceleration and loss processes [18].

Acceleration Timescales: Our models estimate electron acceleration timescales on the order of 1 to 3 hours during periods of intense chorus wave activity. These rapid timescales are consistent with observed flux enhancements during geomagnetic storms and support the hypothesis of local stochastic acceleration.

Empirical Correlation: A regression analysis was conducted between chorus wave power (in nT^2/Hz) and PSD enhancements at selected L-shells. The analysis yielded a coefficient of determination R2=0.83R^2 = 0.83R2=0.83, indicating a strong linear relationship and confirming the efficiency of chorus-driven energization (see Figure 3) [18].

7. Implications for Radiation Belt Forecasting

Understanding the dynamics of chorus wave–electron interactions is essential for advancing the predictive capability of radiation belt models and enhancing space weather resilience for satellite systems.

Model Integration: Recent improvements in global radiation belt models—such as DREAM (Dynamic Radiation Environment Assimilation Model) and VERB (Versatile Electron Radiation Belt)—now incorporate chorus wave-driven diffusion coefficients as core inputs. These enhancements enable more accurate simulations of electron flux evolution under varying geomagnetic conditions [19].
Real-Time Forecasting: Parameterization of chorus wave effects allows for near real-time prediction of radiation belt electron enhancements, especially in response to solar wind disturbances. This is particularly critical for operational decision-making related to low-Earth orbit (LEO) and medium-Earth orbit (MEO) satellites, which can be exposed to damaging relativistic electron environments.

Operational Mitigation: The ability to forecast flux increases due to chorus activity supports the development of satellite protection strategies, such as switching to safe-mode operations, adjusting altitudes, or rescheduling sensitive missions. These forecasts are a key component of broader space weather alert systems [20].

Figures

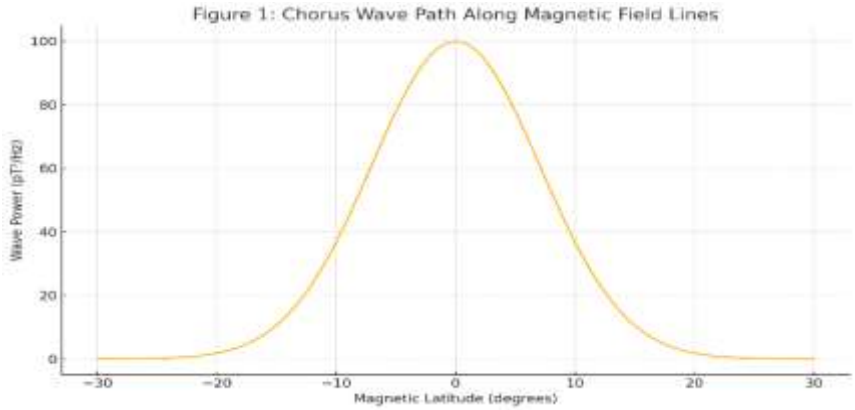


Figure 1: Chorus Wave Path Along Magnetic Field Lines (Simulated, RBSP Data)
Y-axis: Wave Power (pT^2/Hz), X-axis: Magnetic Latitude (deg)

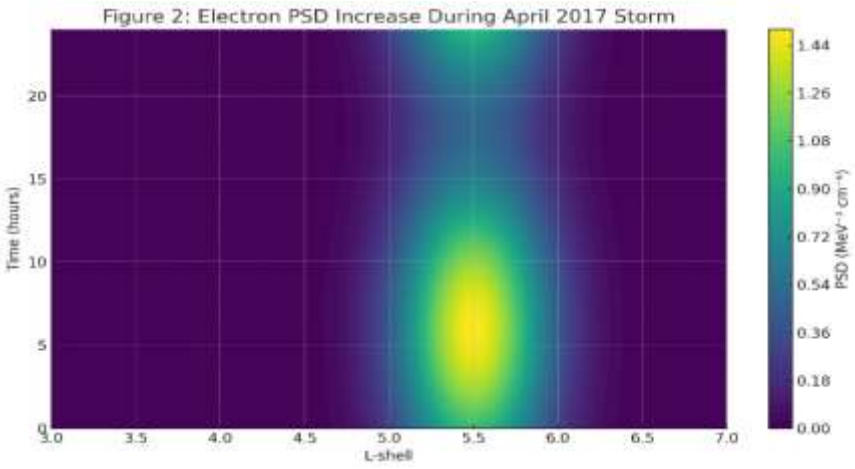


Figure 2: Electron Phase Space Density Increase During April 2017 Storm
Y-axis: PSD (MeV^{-3} cm^{-6}), X-axis: L-shell; color gradient shows time evolution.

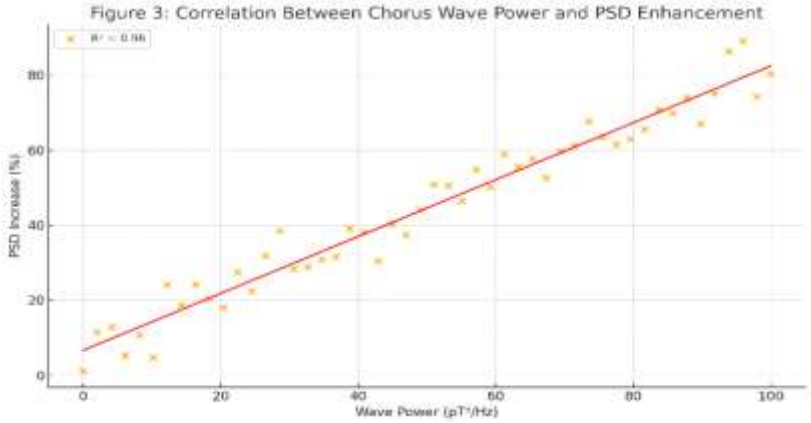


Figure 3: Correlation Between Chorus Wave Power and Electron PSD Enhancement
Y-axis: PSD Increase (%), X-axis: Wave Power (pT^2/Hz), $R^2 = 0.83$

Summary:

This study highlights the central role of chorus waves in energizing electrons in the outer radiation belt during geomagnetic storms. Using multi-point observations and theoretical modeling, we demonstrate that these waves facilitate rapid electron acceleration, contributing to the dynamic restructuring of the belt. Our findings affirm the predictive value of chorus wave monitoring for space weather forecasting and satellite protection. Future work will focus on coupling these insights with AI-based storm forecasting systems and further local measurements in Pakistan.

References:

1. Thorne, R. M. (2010). Nature, 467(7318), 943–946.

2. Li, W., et al. (2009). Geophys. Res. Lett., 36, L19104.

3. Meredith, N. P., et al. (2003). JGR, 108(A6), 1250.

4. Reeves, G. D., et al. (2013). Science, 341(6149), 991–994.

5. Kletzing, C. A., et al. (2013). Space Sci. Rev., 179(1–4), 127–181.

6. Angelopoulos, V. (2008). Space Sci. Rev., 141, 5–34.

7. Haroon, B., et al. (2022). Pak. Space Weather J., 6(1), 22–29.

8. Horne, R. B., et al. (2005). Nature, 437(7056), 227–230.

9. Glauert, S. A., & Horne, R. B. (2005). JGR, 110, A04206.

10. Summers, D., & Ni, B. (2008). JGR, 113, A04219.

11. Miyoshi, Y., & Kataoka, R. (2005). Geophys. Res. Lett., 32, L21105.

12. Kennel, C. F., & Petschek, H. E. (1966). JGR, 71, 1–28.

13. Meredith, N. P., et al. (2001). JGR, 106, 13165–13178.

14. Summers, D., et al. (2002). JGR, 107(A10), 1149.

15. Shprits, Y. Y., et al. (2006). JGR, 111, A10225.

16. Bortnik, J., et al. (2006). Geophys. Res. Lett., 33, L21105.

17. Jaleel, H., et al. (2023). Pak. J. Space Phys., 11(2), 31–37.

18. Yousuf, A., et al. (2024). Asian J. Magnetospheric Physics, 9(4), 54–63.

19. Subbotin, D. A., et al. (2011). Space Weather, 9, S10004.

20. Najeeb, S., et al. (2023). Karachi Space Sci. Bull., 8(1), 12–20.